

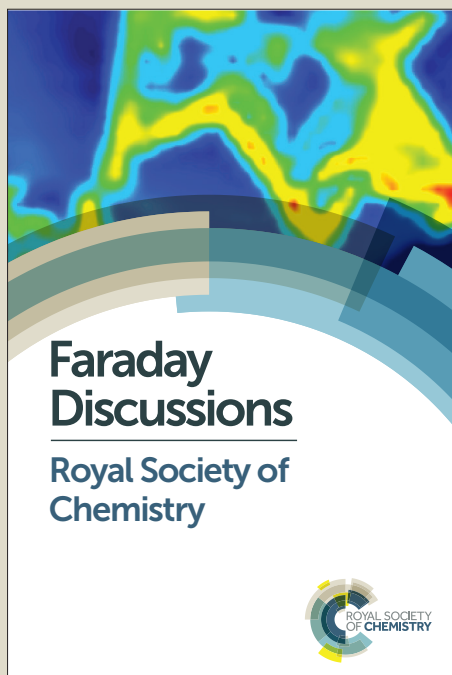
# Faraday Discussions

Accepted Manuscript



This manuscript will be presented and discussed at a forthcoming Faraday Discussion meeting. All delegates can contribute to the discussion which will be included in the final volume.

**Register now to attend!** Full details of all upcoming meetings: <http://rsc.li/fd-upcoming-meetings>



This is an *Accepted Manuscript*, which has been through the Royal Society of Chemistry peer review process and has been accepted for publication.

*Accepted Manuscripts* are published online shortly after acceptance, before technical editing, formatting and proof reading. Using this free service, authors can make their results available to the community, in citable form, before we publish the edited article. We will replace this *Accepted Manuscript* with the edited and formatted *Advance Article* as soon as it is available.

You can find more information about *Accepted Manuscripts* in the [Information for Authors](#).

Please note that technical editing may introduce minor changes to the text and/or graphics, which may alter content. The journal's standard [Terms & Conditions](#) and the [Ethical guidelines](#) still apply. In no event shall the Royal Society of Chemistry be held responsible for any errors or omissions in this *Accepted Manuscript* or any consequences arising from the use of any information it contains.



Journal Name

ARTICLE

## Developing Energy Efficient Lignin Biomass Processing – Towards Understanding Mediator Behaviour in Ionic Liquids

Majd Eshtaya,<sup>a</sup> Andinet Ejigu,<sup>b</sup> Gill Stephens,<sup>a</sup> Darren A. Walsh,<sup>b</sup> George Z. Chen<sup>a, c</sup> and Anna K. Croft<sup>a</sup>

Received 00th January 20xx,  
Accepted 00th January 20xx

DOI: 10.1039/x0xx00000x

www.rsc.org/

Environmental concerns have brought attention to the requirement for more efficient and renewable processes for chemicals production. Lignin is the second most abundant natural polymer, and might serve as a sustainable resource for manufacturing fuels and aromatic derivatives for the chemicals industry after being depolymerised. In this work, the mediator, 2,2'-azino-bis(3-ethylbenthiazoline-6-sulfonic acid) diammonium salt (ABTS), commonly used with enzyme degradation systems, has been evaluated by means of cyclic voltammetry (CV) for enhancing the oxidation of the non-phenolic lignin model compound veratryl alcohol and three types of lignin (organosolv, Kraft and liginosulfonate) in the ionic liquid 1-ethyl-3-methylimidazolium ethyl sulfate,  $[\text{C}_2\text{mim}][\text{C}_2\text{SO}_4]$ . The presence of either veratryl alcohol or organosolv lignin increased the second oxidation peak of ABTS under select conditions, indicating the ABTS-mediated oxidation of these molecules at high potentials in  $[\text{C}_2\text{mim}][\text{C}_2\text{SO}_4]$ . Furthermore, CV was applied as a quick and efficient way to explore the impact of water in the ABTS-mediated oxidation of both organosolv and liginosulfonate lignin. Higher catalytic efficiencies of ABTS were observed for liginosulfonate solutions either in sodium acetate buffer or when  $[\text{C}_2\text{mim}][\text{C}_2\text{SO}_4]$  (15 v/v%) was present in the buffer solution, whilst there was no change found in the catalytic efficiency of ABTS in  $[\text{C}_2\text{mim}][\text{C}_2\text{SO}_4]$ - liginosulfonate mixtures relative to ABTS alone. In contrast, organosolv showed an initial increase in oxidation, followed by a significant decrease on increasing the water content of a  $[\text{C}_2\text{mim}][\text{C}_2\text{SO}_4]$  solution.

### Introduction

Lignin is the second most abundant naturally synthesised compound after cellulose comprising 15–30% of total dry wood. It is a complex natural polymer composed of a diversely linked network of phenolic and non-phenolic compounds and hence could provide a potential source for the sustainable production of fuels and aromatic chemicals that are currently obtained from petroleum-based feedstocks.<sup>1–3</sup> Currently, lignin is produced mainly as a major by-product of both the pulp and paper industry and biomass ethanol industry, and is either discharged in black liquor or used as a low-grade fuel. Therefore, depolymerisation of lignin into aromatic products would greatly benefit both the fine chemicals industry and the further development of sustainable chemical processes.<sup>4–6</sup>

Over the years, several methods have been explored and documented for the depolymerisation of lignin, such as pyrolysis,<sup>4, 7</sup> chemical oxidation including electrochemical oxidation,<sup>6, 8, 9</sup> hydrolysis<sup>10, 11</sup> and enzymatic reactions.<sup>12–14</sup> Among these methods, enzymatic reactions and electrochemical

oxidation are preferable due to their environmentally friendly characteristics and lower energy demands.

A number of different types of enzymes are available for the biodegradation of lignin, such as laccase (EC 1.10.3.2, *p*-benzenediol: dioxygen oxidoreductases).<sup>15</sup> Laccases alone have only a very limited effect on lignin degradation due to their low redox potentials (0.45–0.80 V vs. NHE). This means that laccases can oxidise phenolic groups only, but not the non-phenolic aromatic structures that comprise more than 80% of lignin. Laccases can react indirectly with non-phenolic compounds and potentially degrade lignin in the presence of a redox mediator.<sup>16</sup> A mediator is low-molecular weight compound that, once oxidised by the enzyme, diffuses away from the enzymatic pocket and then can oxidise other substrates, thus regenerating its reduced form. Overall, the laccase-mediator system acts as a catalyst to assist oxidation of lignin by mediation of electron transfer from the oxidisable groups in lignin to oxygen molecules. This simplified mechanism is depicted in Figure 1a.<sup>16–21</sup> Generally, the ideal redox mediator should be a good laccase substrate, able to generate stable radicals upon oxidation that do not inhibit the enzymatic reaction, and also should not be consumed during the redox transformation.<sup>17, 19, 22</sup>

In the past two decades, the range of compounds identified as mediators for the laccase mediator system (LMS) has increased dramatically and 2,2'-azino-bis(3-ethylbenthiazoline-6-sulfonic acid)

<sup>a</sup> Department of Chemical and Environmental Engineering, Faculty of Engineering, University of Nottingham, Nottingham NG7 2RD, UK

<sup>b</sup> Department of Chemistry, University of Nottingham, Nottingham NG7 2RD, UK

<sup>c</sup> Department of Chemical and Environmental Engineering, Faculty of Science & Engineering, University of Nottingham Ningbo China, Ningbo 315100, P. R. China.

diammonium salt **1** (ABTS) (Figure 2) is currently regarded as the best mediator for laccase.<sup>21-26</sup>

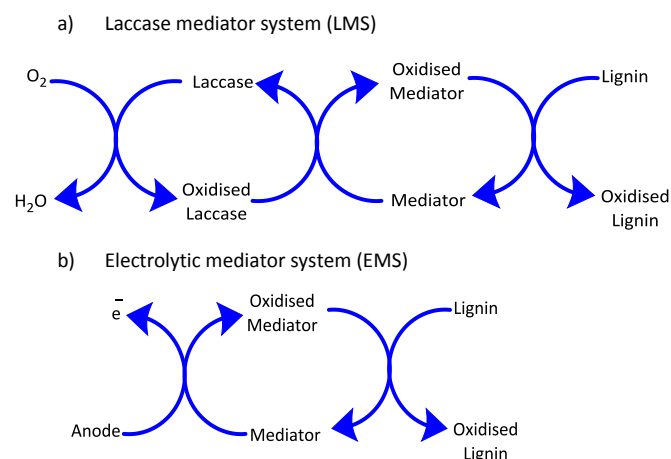


Figure 1: Laccase mediator system (LMS) and electrolytic mediator system (EMS)<sup>27</sup>

Despite the obvious advantages, LMS has a number of drawbacks such as high cost of the enzymes and their sensitivity to the experimental conditions (pH, temperature and inhibitors). In addition, there are difficulties associated with the use of LMS in conventional solvents.<sup>28-31</sup>

In contrast to LMS, an electrolytic mediator system (EMS) (Figure 1b) could provide a promising and effective alternative for lignin depolymerisation. Instead of using a laccase to oxidise the mediator, the mediator can be oxidised electrochemically instead. By avoiding the requirement for a sensitive enzyme, the electrochemical process can be performed under a wide range of pH and temperature conditions with mediators that have a high redox potential.<sup>17, 19, 27</sup>

One of the main obstacles to the degradation of lignin is its insolubility in most commonly-used solvents. Over recent years, ionic liquids (ILs) have been used for the dissolution of biomass. Very high solubility of lignin has been achieved using 1-ethyl-3-methylimidazolium acetate ( $[C_2mim][C_1CO_2]$ ), 1-butyl-3-methylimidazolium chloride ( $[C_4mim]Cl$ ) and 1-ethyl-3-methylimidazolium ethyl sulfate ( $[C_2mim][C_2SO_4]$ ),<sup>32-34</sup> and this good solubility provides new opportunities for lignin degradation.

Unlike conventional organic solvents, room temperature ILs have many favourable properties in electro-organic synthesis including low vapour pressure at room temperature, a wide liquid range, inherent conductivity, non-volatility, good dissolving power towards many substrates, and excellent thermal and chemical stability. Also, they possess a wide window of electrode potential and no addition of supporting electrolyte is required, which can assist electrochemical processes such as the oxidation of lignin.<sup>35, 36</sup> When compared to conventional solvents, however, ILs are commonly 10–100 times more viscous, and the diffusion rates of species in these media are lowered accordingly.<sup>36, 37</sup>

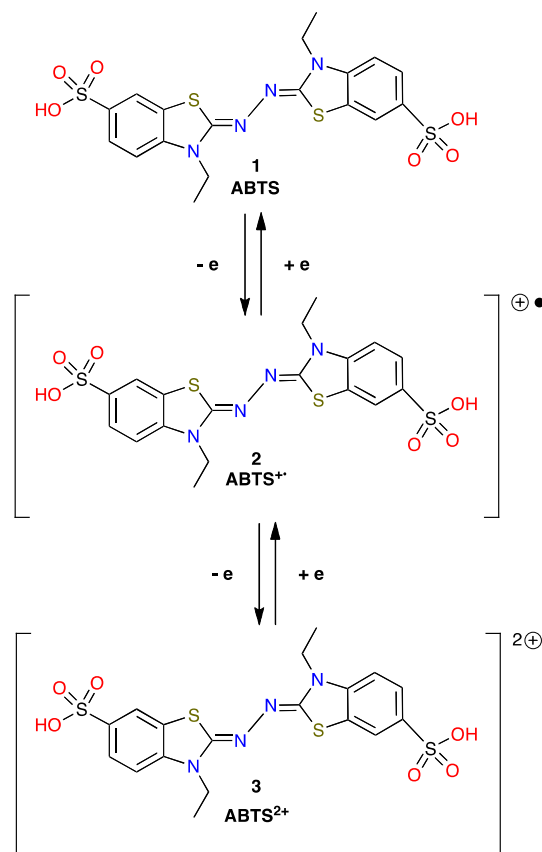


Figure 2: Chemical structure of ABTS mediator and formation of the cation radical and the dication by removal of one and two electrons from ABTS.<sup>24</sup>

Numerous studies have been done on the electrochemical behaviour of ABTS **1** in aqueous solutions<sup>21-27, 38</sup> but to our knowledge, no study of the electrochemical behaviour of ABTS **1** for oxidising either lignin or a lignin model compound in ionic liquids has so far been reported. More recently, Reichert and co-workers successfully depolymerised alkali lignin through electro-catalytic oxidative cleavage without using any mediator. They performed the depolymerisation in a special protic ionic liquid, triethylammonium methanesulfonate ( $[HN_{222}][C_1SO_3]$ ), using an active electrode of mixed ruthenium/vanadium/titanium oxides. A wide range of aromatic compounds, such as aldehydes and ketones were identified as the cleavage products, as detected by GC-MS and HPLC after diethyl ether extraction.<sup>6</sup> Another study performed by Zhu *et al.*<sup>9</sup> achieved electro-oxidative cleavage of lignin in alkaline solutions (2 wt %) by anodic oxidation coupled with electro-generated  $H_2O_2$  oxidation in a non-diaphragm electrolytic cell. Owing to the effective breakage of the C–C and C–O–C linkages among C9 units, lignin macromolecules were depolymerised into low molecular weight aromatic products with different functional groups, such as aldehydes, ketones, phenols and acids.

This work is aimed at studying the electrochemical behaviour of ABTS **1** in oxidising the non-phenolic lignin model veratryl alcohol **4** and three technical lignins: Kraft lignin, organosolv lignin and sulfonated lignin (lignosulfonate), in  $[C_2mim][C_2SO_4]$ . Due to its high capacity to dissolve lignin,  $[C_2mim][C_2SO_4]$  was chosen in this study.<sup>39, 40</sup> Cyclic voltammetry was applied as a quick, accurate and efficient way to explore the ABTS-mediated oxidation process.

## 2. MATERIALS AND METHODS

### 2.1 Chemicals

Organosolv Lignin was supplied by Lignol Innovations Ltd, Canada. The ionic liquid  $[C_2mim][C_2SO_4]$  ( $\geq 95\%$  purity), sodium lignosulfonate, alkali (Kraft) lignin, 3,4-dimethoxybenzyl alcohol **4** (veratryl alcohol), silver trifluoromethane sulfonate ( $AgTfO$ ) ( $\geq 98\%$  purity), 2,2'-azino-bis-(3-ethylbenzothiazoline-6-sulfonic acid) diammonium salt **1** (ABTS) and all other chemicals and solvents used in this study were purchased from Sigma Aldrich (UK) and used without any further purification.

### 2.2 Viscosity Measurements

The viscosities of  $[C_2mim][C_2SO_4]$ , 0.1 M sodium acetate buffer solution (pH 4.5), 15% (v/v)  $[C_2mim][C_2SO_4]$ /buffer solution and lignin/ $[C_2mim][C_2SO_4]$  mixtures were measured at room temperature with a Kinexus pro<sup>+</sup> rotational rheometer (Malvern Instruments Ltd., UK) equipped with cone-and-plate geometry (40 mm in diameter; with a cone angle of 4° and a gap of 150  $\mu m$ ). A strain rate sweep was performed from 1.0 to 1000  $s^{-1}$ .

### 2.3 Cyclic Voltammetry (CV) Measurements

Cyclic voltammetry and chronoamperometry were carried out using Autolab Type III potentiostat/galvanostat from EcoChemie (Metrohm, Netherlands) controlled by the Autolab GPES software, version 4.9, in an undivided three-electrode cell. A glassy carbon (GC) disc electrode (3.0 mm in diameter) was used as the working electrode, which was polished prior to use and between each measurement using aqueous alumina (0.05  $\mu m$ ) suspensions. After polishing, the electrode surface was rinsed with deionised water. The reference electrode was an IL-based  $Ag/Ag^+$  electrode, which has been described previously (10 mM  $AgTfO$ ,  $[C_2mim][C_2SO_4]$ )<sup>41</sup> and a graphite rod as the counter electrode. All the solutions were degassed with nitrogen prior to measuring and all experiments were performed at room temperature.

The electrochemical characterisation of ABTS **1** was first carried out alone in either 0.1 M sodium acetate buffer solution (pH 4.5), 15% (v/v)  $[C_2mim][C_2SO_4]$ /buffer solution or as-received  $[C_2mim][C_2SO_4]$  at different scan rates. The voltammetric responses of ABTS mediator **1** were also recorded separately at the same potential scan rate in the presence of either the lignin model compound veratryl alcohol **4** (13.8 mM) in 15% (v/v)  $[C_2mim][C_2SO_4]$ /buffer solution or as-received  $[C_2mim][C_2SO_4]$ , or lignin (Kraft, organosolv and lignosulfonate) (5 wt %) dissolved in as-received  $[C_2mim][C_2SO_4]$ . The current response of ABTS-mediated organosolv lignin at different concentrations of sodium phosphate buffer (pH 12) in  $[C_2mim][C_2SO_4]$  was also measured. Finally, the voltammograms of the ABTS **1** in the presence of lignosulfonate, either in sodium acetate buffer solution or in 15% (v/v)  $[C_2mim][C_2SO_4]$ /buffer solution, were recorded.

## 3. RESULTS AND DISCUSSION

### 3.1 Electrochemical behaviour of ABTS in $[C_2mim][C_2SO_4]$

The cyclic voltammogram of 10 mM ABTS **1** in  $[C_2mim][C_2SO_4]$  with a scan rate of 200 mV/s is shown in Figure 3. Two oxidation peaks ( $E_{p,a}$ ) at potentials of 0.500 V (A) and 0.815 V (B) were observed,

corresponding to the oxidation of ABTS **1** to its cation radical **2** ( $ABTS^{\cdot+}$ ) and subsequently to its dication **3** ( $ABTS^{2+}$ ). The reverse scan showed two reduction peaks ( $E_{p,c}$ ) at 0.738 V (C) and 0.423 V (D) for the reduction of the dication and the cation radical, respectively. Analysis of the two redox couples at a range of scan rates (see inset in Figure 3) revealed that the oxidation ( $i_{p,a}$ ) and reduction ( $i_{p,c}$ ) peak currents were proportional to the square root of the scan rate. Additionally, at each scan rate, the ratio of  $i_{p,a}$  to  $i_{p,c}$  was close to one, indicating that the mass transport of ABTS **1** to the electrode surface was diffusion controlled in  $[C_2mim][C_2SO_4]$  and confirmed that the radical cation  $ABTS^{\cdot+}$  **2**, dication  $ABTS^{2+}$  **3** and  $[C_2mim][C_2SO_4]$  do not interact with one another, e.g. *via* ion pairing or proton transfer, to a significant extent. These observations are consistent with the electrochemical behaviour of ABTS in aqueous systems reported by Bourbonnais *et al.*<sup>21</sup>

For an electrochemically-reversible reaction with a one-electron transfer process, the peak-peak potential separation ( $\Delta E_p = E_{p,a} - E_{p,c}$ ) for each redox couple at each scan rate should be approximately 59 mV at room temperature and independent of the scan rate. However, the  $\Delta E_p$  for the ABTS radical cation **2** and dication **3** in  $[C_2mim][C_2SO_4]$  were significantly greater than 59 mV and increased as the scan rate increased (77 mV at 50 mV/s and 101 mV at 1000 mV/s), indicating a quasi-reversible redox process. These results might indicate slow electron transfer kinetics, and may also be partly attributed to the effect of uncompensated ohmic resistance of the electrolyte and the measuring circuit.<sup>42</sup>

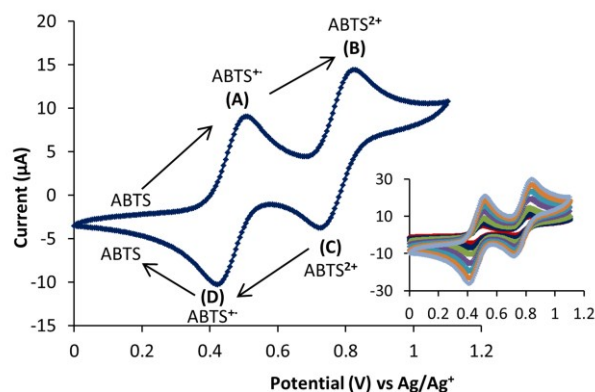


**Figure 3:** Cyclic voltammogram of 10 mM ABTS **1** in  $[C_2mim][C_2SO_4]$  recorded at a scan rate of 200 mV/s. The inset shows the cyclic voltammogram of 10 mM ABTS **1** in  $[C_2mim][C_2SO_4]$  with varying scan rates (from inside to outside (mV/s): 50, 100, 200, 400, 600, 800 and 1000).

The CV features observed at high (200 mV/s) and low (50 mV/s) scan rates differed markedly, as shown in Figure 4. Thus, at a low scan rate and a higher concentration of ABTS (50 mM), no cathodic signal corresponding to the reduction of the ABTS dication **3** was detected. Instead, the intensity of the  $ABTS^{\cdot+}$  **2** reduction peak was about 1.4 fold that of its oxidation peak ( $i_{p,a}/i_{p,c}=1.4$ ). This behaviour was previously observed in aqueous solutions and attributed to the comproportionation reaction between ABTS **1** and its dication **3** with the formation of  $ABTS^{\cdot+}$  **2**, which has resulted in the disappearance of a cathodic peak due to the reduction of  $ABTS^{2+}$  **3**.<sup>21</sup> This comproportionation reaction depends on the concentration of the electroactive species close

to the surface of the electrode so that, in the case when the concentration of ABTS **1** is high, the comproportionation reaction of the dication **3** will take place before its reduction at the electrode surface.

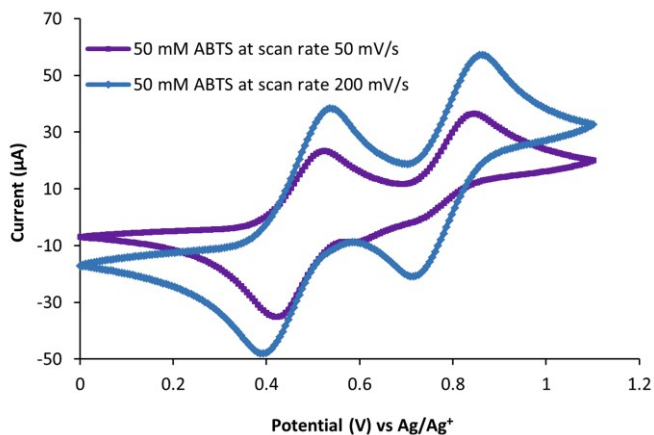


**Figure 4:** Cyclic voltammograms of 50 MABTS in [C<sub>2</sub>mim][C<sub>2</sub>SO<sub>4</sub>] recorded at scan rates of 50 mV/s and 200 mV/s.

#### Diffusion coefficient of ABTS in [C<sub>2</sub>mim][C<sub>2</sub>SO<sub>4</sub>]

The impact of solvent viscosity on the oxidation reaction can be related to the diffusivity of the substrate. Single potential step chronoamperometry was employed in order to determine the diffusion coefficient of ABTS **1** in [C<sub>2</sub>mim][C<sub>2</sub>SO<sub>4</sub>]. Figure 5A shows a typical chronoamperogram obtained using 10.0 mM ABTS **1** in [C<sub>2</sub>mim][C<sub>2</sub>SO<sub>4</sub>] after a potential step from a potential where no faradaic reaction occurred to a potential at which the oxidation of ABTS **1** was diffusion controlled. The current, *i*, is proportional to *t*<sup>-0.5</sup> as shown by the Cottrell equation, equation (1)

$$i(t) = \frac{nFACD^{0.5}}{\pi^{0.5}t^{0.5}} \quad (1)$$

where *i* is the peak current, *n* the number of electrons transferred/molecule, *A* the electrode surface area, *C* the bulk concentration of the redox species, *D* the Diffusion coefficient of the redox species and *F* the Faraday constant. Figure 5B shows the corresponding Cottrell profile of *i(t)* vs *t*<sup>0.5</sup> and, from the gradient of the straight line best-fit to the plot, the diffusion coefficient of ABTS **1**/ABTS<sup>2+</sup> **2** in [C<sub>2</sub>mim][C<sub>2</sub>SO<sub>4</sub>] was calculated to be 1.9 (± 0.3) × 10<sup>-8</sup> cm<sup>2</sup>s<sup>-1</sup>, which is typical for molecular species in viscous ILs.<sup>42,43</sup> A similar analysis was performed to find the diffusion coefficients of ABTS **1** in sodium acetate buffer solution and the 15% (v/v) [C<sub>2</sub>mim][C<sub>2</sub>SO<sub>4</sub>]/buffer mixture (Table 1). Table 1 also shows the viscosity of these solvents. There was a good agreement between the diffusion coefficients of ABTS **1** and the viscosity of both buffer solutions and [C<sub>2</sub>mim][C<sub>2</sub>SO<sub>4</sub>] with literature values.<sup>42,44</sup> The value of the diffusion coefficient of ABTS **1** in [C<sub>2</sub>mim][C<sub>2</sub>SO<sub>4</sub>] was almost three orders of magnitude lower than that determined in the buffer solution (3.5 (± 0.2) × 10<sup>-6</sup>), which is consistent with the high viscosity of this IL and reflects the low mass transport rate of the ABTS **1** in [C<sub>2</sub>mim][C<sub>2</sub>SO<sub>4</sub>], compared to that in the buffer solution.

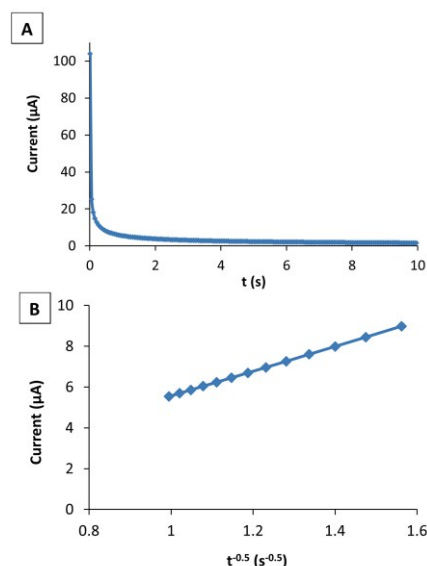


**Figure 5:** (A) Potential step chronoamperogram obtained at a 3 mm diameter glassy carbon (GC) disk electrode in 10.0 mM ABTS **1** in [C<sub>2</sub>mim][C<sub>2</sub>SO<sub>4</sub>]. The potential was stepped from 0.3 V to 0.6 V vs. ABTS **1**/ABTS<sup>2+</sup> **2** and held for 10 s. (B) Cottrell plot of *i(t)* vs. *t*<sup>0.5</sup> for the oxidation process.

**Table 1:** Diffusion coefficients of ABTS **1** in different solvents using potential step chronoamperometry.

Solution type	Diffusion Coefficient (cm <sup>2</sup> s <sup>-1</sup> )	Viscosity (mPa.s)
1 mM ABTS in sodium acetate buffer	3.5 (± 0.2) × 10 <sup>-6</sup>	0.76 ± 0.02
1 mM ABTS in 15% (v/v) [C <sub>2</sub> mim][C <sub>2</sub> SO <sub>4</sub> ]/Buffer	1.74 (± 0.04) × 10 <sup>-6</sup>	1.23 ± 0.01
1 mM ABTS in [C <sub>2</sub> mim][C <sub>2</sub> SO <sub>4</sub> ]	2.6 (± 0.1) × 10 <sup>-8</sup>	96.6 ± 4.4
10 mM ABTS in [C <sub>2</sub> mim][C <sub>2</sub> SO <sub>4</sub> ]	1.9 (± 0.3) × 10 <sup>-8</sup>	96.6 ± 4.4

### 3.2 Cyclic Voltammetry of Veratryl Alcohol (VA)

The redox reaction between the mediator, ABTS **1** and the non-phenolic lignin model compound veratryl alcohol **4** (VA) was also included in this study as a benchmark, using CV. As can be seen in Figure 6, VA **4** alone did not show any oxidation peak below 900 mV but, in the presence of ABTS **1**, the recorded peak height increased by more than four-fold at the appropriate potential, indicating the ABTS<sup>2+</sup> dication **3** catalysing VA **4** oxidation. No oxidation of this lignin model **4** occurred in the potential range corresponding to the formation of the ABTS<sup>2+</sup> **2** between 0.70 and 0.95 V. This CV finding is consistent with those previously reported in the literature.<sup>37</sup> The effect of VA **4** on redox catalysis of an electrochemical reaction, as described by Bourbonnais *et al.*,<sup>21</sup> (Scheme 1) is for the ABTS dication **3** to oxidise the VA **4** to veratryl aldehyde **5** with concurrent regeneration of the ABTS radical **2**, resulting in an increase in the peak current compared to that seen on the CV of the ABTS solution without veratryl alcohol **4**.

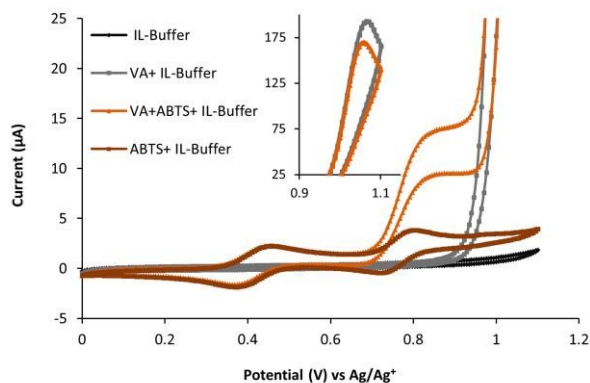
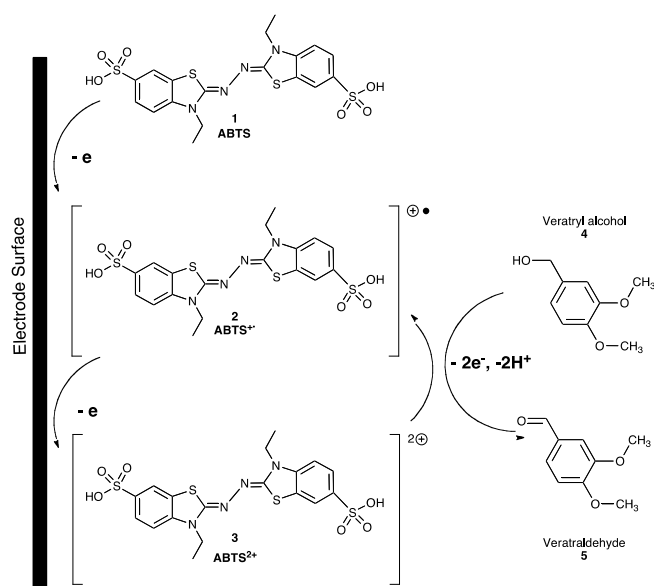


**Figure 6:** Cyclic voltammograms of 1 mM ABTS **1**, 13.8 mM veratryl alcohol **4**, 13.8 mM veratryl alcohol **4** mixed with 1 mM ABTS **1** in 15% (v/v)  $[\text{C}_2\text{mim}][\text{C}_2\text{SO}_4]$  in 0.1 M sodium acetate buffer (pH 4.5) recorded at a scan rate of 10 mV/s. The inset shows the portion of the CVs with current above 25  $\mu\text{A}$  between 0.9 and 1.1 V.



**Scheme 1:** Schematic representation of the reaction of ABTS **1** and VA **4** at the working electrode

The electrochemical behaviour of ABTS **1** in the presence of VA **4** in as-received  $[\text{C}_2\text{mim}][\text{C}_2\text{SO}_4]$  was also explored. Figure 7 shows the CVs of ABTS **1** (1.0 mM), veratryl alcohol **4** (13.8 mM) and the two compounds mixed together in  $[\text{C}_2\text{mim}][\text{C}_2\text{SO}_4]$  under the same conditions as described above for the 15% (v/v)  $[\text{C}_2\text{mim}][\text{C}_2\text{SO}_4]$ /buffer mixture. The resulting CVs confirm the stability of  $[\text{C}_2\text{mim}][\text{C}_2\text{SO}_4]$  in the oxidative potential range of 0 to 1.1 V vs  $\text{Ag}/\text{Ag}^+$ . As with the 15% (v/v)  $[\text{C}_2\text{mim}][\text{C}_2\text{SO}_4]$ /buffer mixture, the simultaneous electrochemical oxidation of ABTS **1** and VA **4** resulted in an increase of the second oxidation peak of ABTS, indicating a regeneration of ABTS **1** at the electrode. However, the peak current of the second oxidation in the presence of the VA **4** is reduced by 10 fold in the  $[\text{C}_2\text{mim}][\text{C}_2\text{SO}_4]$ , compared with in 15% (v/v)  $[\text{C}_2\text{mim}][\text{C}_2\text{SO}_4]$ /buffer mixture as can be seen by comparing Figures 6 and 7. This is probably due to the high viscosity of  $[\text{C}_2\text{mim}][\text{C}_2\text{SO}_4]$  (96.6 mPa.s at 22 °C, Table 1), and can be explained by VA **4** diffusion through the

higher viscosity solvent becoming slower and hindering the transport of analytes towards the working electrode. Therefore, lower peak currents were measured. Figures 6 and 7 also indicate that the electrochemical behaviour of ABTS **1** in the  $[\text{C}_2\text{mim}][\text{C}_2\text{SO}_4]$  was different to that found in 15% (v/v)  $[\text{C}_2\text{mim}][\text{C}_2\text{SO}_4]$ /buffer mixtures. Whereas the ABTS **1** showed reversible electrochemical behaviour in 15% (v/v)  $[\text{C}_2\text{mim}][\text{C}_2\text{SO}_4]$ /buffer mixtures, the CVs of ABTS **1** in the  $[\text{C}_2\text{mim}][\text{C}_2\text{SO}_4]$  did not show the cathodic peak corresponding to the reduction of the dication **3** ( $\text{ABTS}^{2+}$ ) at this particular ABTS **1** concentration and at the scan rate used.

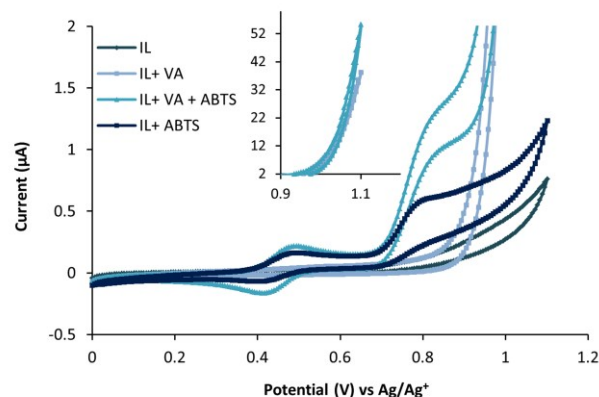


**Figure 7:** Cyclic voltammograms of 1 mM ABTS **1**, 13.8 mM veratryl alcohol **4**, 13.8 mM veratryl alcohol **4** mixed with 1 mM ABTS **1** in  $[\text{C}_2\text{mim}][\text{C}_2\text{SO}_4]$  recorded at a scan rate of 10 mV/s. The inset shows the portion of the CVs with current above 2.0  $\mu\text{A}$  between 0.9 and 1.1 V.

### 3.3 Cyclic voltammetry of Different Lignins in $[\text{C}_2\text{mim}][\text{C}_2\text{SO}_4]$

Mainly because of the structural complexity of lignin (Figure 8), most of the studies reported to date have been performed using lignin model compounds. However, the challenge is to valorise the widely available authentic lignins that are by-products of cellulose isolation. Therefore, the reactions of ABTS **1** with three types of technical lignin (organosolv, Kraft and sulfonated lignin) were studied by cyclic voltammetry in  $[\text{C}_2\text{mim}][\text{C}_2\text{SO}_4]$  to determine the reactivities of the two oxidised states of ABTS, **2** and **3**, towards lignin (from Figure 9 to Figure 12). Initially the voltammetric response of ABTS **1** (10 mM) in  $[\text{C}_2\text{mim}][\text{C}_2\text{SO}_4]$  was assayed alone at different scan rates and then the voltammetric responses of each type of lignin (5 wt %) were also recorded separately at the same potential scan rate. Each lignin (5 wt %) was dissolved in the  $[\text{C}_2\text{mim}][\text{C}_2\text{SO}_4]$  and then, the mixture was stirred at 60 °C for 2 h in order to ensure complete dissolution. Subsequently, nitrogen was purged through the resultant solutions before CVs were measured to reduce potential interference from oxygen. Finally, the CVs of the ABTS **1** (10 mM) in the presence of lignin (5 wt %) in  $[\text{C}_2\text{mim}][\text{C}_2\text{SO}_4]$  were recorded as indicated above.

As can be seen in Figure 9, an increase in the oxidation current was detected at potentials around 1.0 V for all types of lignin in the absence of ABTS **1**. This is possibly related to the oxidation of the hydroxyl (OH) group on either the  $\alpha$ -carbon or  $\gamma$ -carbon (see Figure 8).<sup>36</sup> ABTS **1** behaved differently in response to addition of different lignins, as shown in Figures 10 to 12. Its behaviour was fairly

electrochemically reversible in the presence of lignosulfonate and Kraft lignin in  $[C_2mim][C_2SO_4]$  (Figures 11 and 12). However, organosolv lignin caused a significant increase in the second oxidation peak of ABTS (Figure 10).

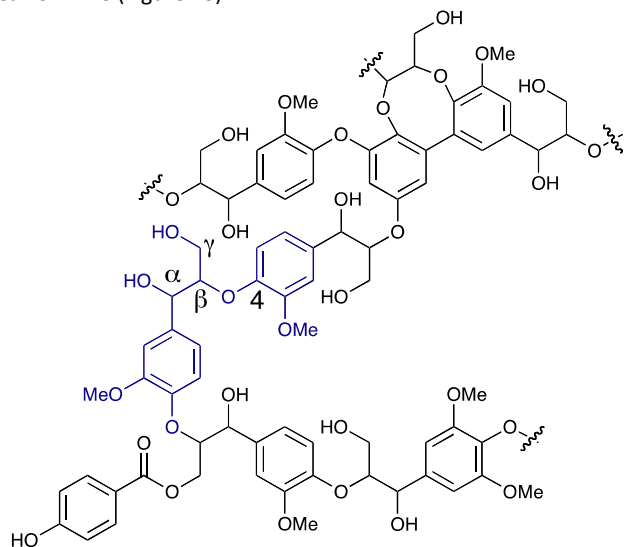


Figure 8: Representative structure of a fragment of lignin.<sup>45</sup>

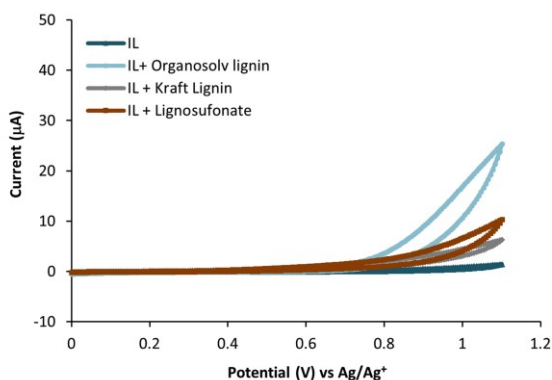


Figure 9: Cyclic voltammograms of organosolv, Kraft and lignosulfonate lignin (5 wt %) in  $[C_2mim][C_2SO_4]$  recorded at a scan rate of 50 mV/s.

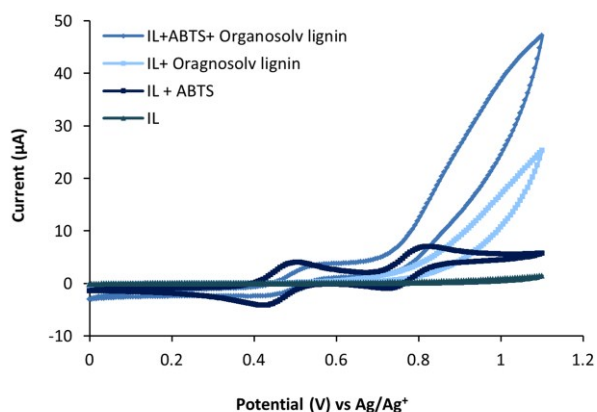


Figure 10: Cyclic voltammograms of ABTS 1 (10 mM), organosolv lignin (5 wt %) and organosolv lignin (5 wt %) mixed with 10 mM ABTS 1 in  $[C_2mim][C_2SO_4]$  recorded at scan rate of 50 mV/s.

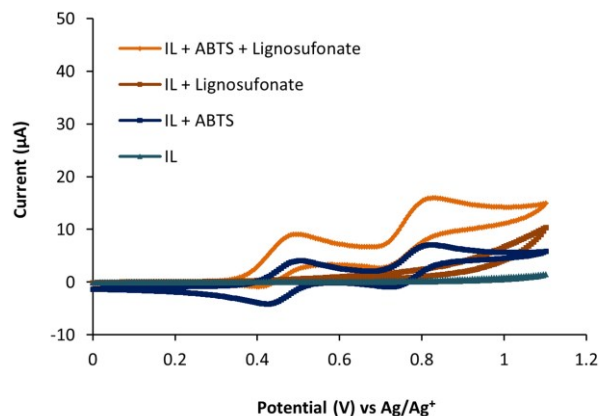


Figure 11: Cyclic voltammograms of ABTS 1 (10 mM), lignosulfonate (5 wt %) and lignosulfonate (5 wt %) mixed with 10 mM ABTS 1 in  $[C_2mim][C_2SO_4]$ , recorded at a scan rate of 50 mV/s.

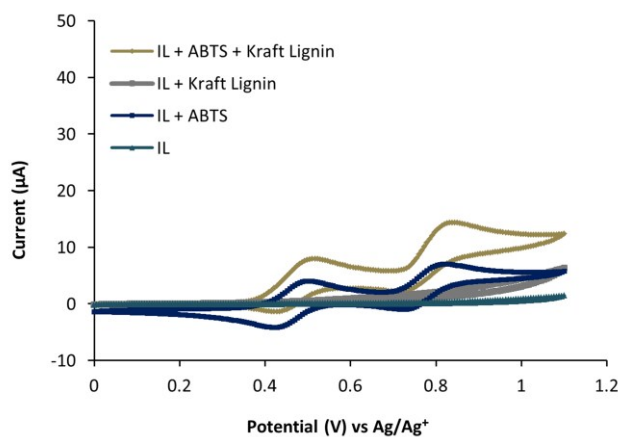


Figure 12: Cyclic voltammograms of ABTS (10 mM), Kraft lignin (5 wt %) and Kraft lignin (5 wt %) mixed with 10 mM ABTS in  $[C_2mim][C_2SO_4]$  recorded at a scan rate of 50 mV/s.

In Figure 10, the anodic current corresponding to formation of the radical cation **2** decreased slightly and shifted towards more positive potentials. These features seem to indicate direct interactions between ABTS and organosolv lignin, which may be due to the high polydispersity of organosolv lignin and the presence of low molecular weight fractions that could activate cascade reactions between their phenolic and non-phenolic structures.<sup>19, 38, 46</sup> Generally, however, organosolv lignin contains less contaminants than lignin obtained from other processes, such as Kraft lignin or lignosulfonate,<sup>47</sup> and is also closest in structure to native lignin.

It can also be seen in Figure 10 that the dication formation current peak seemed to have merged into, and also enhanced the current from oxidation of organosolv lignin. This CV response was highly likely caused by the peak potential for formation of the ABTS dication **3** being very close to the current onset potential for the oxidation of organosolv lignin. Nonetheless, the significantly greater currents between 0.7 and 1.1 V on the CV of the mixed solution of ABTS and organosolv lignin than those on the CVs individually recorded is still evidence for the ABTS dication to be responsible for the mediated or

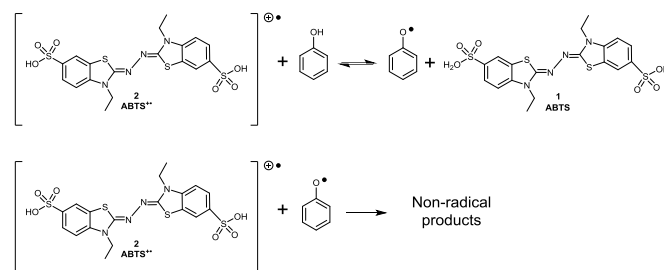
catalytic oxidation of organosolv lignin. A possible factor of influence on the differing oxidation behaviour of organosolv lignin with ABTS **1** is that, because organosolv lignin comprises relatively low molecular weight lignin units, relative to the other lignins examined herein, it is also the most amenable to IL treatment, to afford a more deconstructed lignin, thus making it more accessible to ABTS **1**.<sup>48</sup>

The CVs of ABTS **1** in the presence of liginosulfonate and Kraft lignin were quite similar, as can be seen in Figures 11 and 12. In these two cases, both the peak currents for formation of the radical cation **2** and dication **3** of ABTS increased noticeably after addition of either liginosulfonate or Kraft lignin. These results indicate possible interactions between the lignin and both **2** and **3**, leading to the increase of the oxidation currents. However, in comparison with Figures 6, 7 and 10, whilst these interactions might have caused depolymerisation of the lignin, the effect, if any, was insignificant and controlled by diffusion. It is possibly due to a solubility issue. Organosolv lignin is soluble in  $[C_2mim][C_2SO_4]$  at room temperature, but liginosulfonate and Kraft lignin exhibit low solubility, or the dissolution is kinetically very slow in  $[C_2mim][C_2SO_4]$  at room temperature. A mixing process at 60 °C for about 2 h was needed to make sure these two lignins completely dissolved. This heating step could potentially initiate adverse coupling reactions of the phenols in the lignin structure. Additionally, in contrast to organosolv lignin, Kraft lignin and liginosulfonate contain sulfur groups and therefore, a strong interaction between  $[C_2mim][C_2SO_4]$  and sulfur species on the lignin could have possibly occurred in such a way that it limits accessibility of ABTS **1** to the lignin macromolecules. Thus, further studies are required to understand the intermolecular interactions between the lignin and ABTS mediator **1** with the IL ions to explain the differences between the reactivity of ABTS **1** with each of these types of lignin.

### 3.4 Cyclic Voltammetry of Liginosulfonate (LS)

In order to elucidate the effect of viscosity on the ABTS **1** catalytic efficiency (as defined later), CVs of liginosulfonate in the sodium acetate buffer (pH 4.5) and the 15% (v/v)  $[C_2mim][C_2SO_4]$ /buffer mixtures were studied. Most of the lignins available are practically water insoluble. However, sodium liginosulfonate contains hydrophilic functional groups, which make this type of lignin water-soluble. Therefore, sodium liginosulfonate was used in this part of the study. Figure 13 shows the CV of liginosulfonate (1 wt %) at a low potential scan rate (10 mV/s) in the 15% (v/v)  $[C_2mim][C_2SO_4]$ /buffer solution. The increase in the anodic peak currents of ABTS **1** in presence of liginosulfonate, compared with those measured in the presence of ABTS alone, indicate that both the cation radical **2** and dication **3** were involved in the redox reactions of liginosulfonate. This finding is consistent with the results obtained by Bourbonnais and co-workers for electrochemical oxidation of Kraft lignin (Indulin) in buffer solutions.<sup>17, 21</sup> The increase of the peak current for formation of the ABTS cation radical **2** has been related to the quantity of more easily oxidisable residues in lignin such as phenolic groups, whereas the increase of the peak current for formation of the ABTS dication **3** corresponds more likely to (non-phenolic) groups in lignin with higher redox potentials.<sup>49</sup> The reaction mechanism is already known for the oxidation of phenols by ABTS cation radical **2** and consists of at least two homogeneous chemical reactions: fast and reversible electron

transfer (Scheme 2), consistent with the increase in the cation radical peak in Figure 13, followed by the reaction of the formed phenoxy radicals with another ABTS-derived radical cation.<sup>44, 50</sup>



**Scheme 2:** Proposed reaction scheme for the oxidation of phenol with ABTS cation radical **2**.

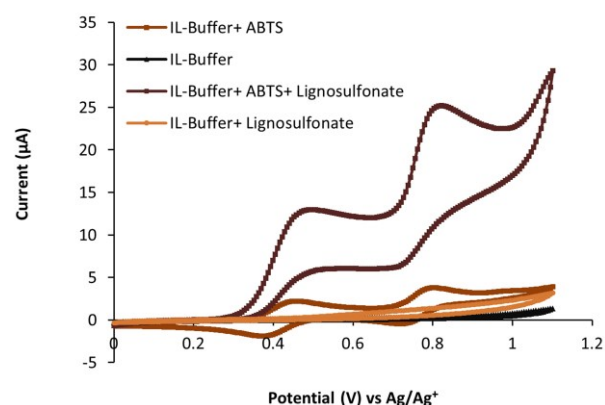


**Figure 13:** Cyclic voltammograms of 1 mM ABTS, 1 wt % liginosulfonate, 1 wt % liginosulfonate mixed with 1 mM ABTS in 15% (v/v)  $[C_2mim][C_2SO_4]$  in 0.1 M sodium acetate buffer (pH 4.5) recorded at a scan rate of 10 mV/s.

Additionally, in the presence of liginosulfonate the CVs present well-shaped oxidation peaks (Figure 13), but only one small reduction peak was observed, indicating absence of ABTS **1** regeneration. A likely explanation is that a portion of the ABTS dication **3**, and almost all of the radical cation **2** formed, coupled with phenoxy radicals and other reactive intermediates produced during the reaction to form covalently-linked derivatives.<sup>51</sup>

The catalytic efficiency of ABTS **1** can be expressed by the ratio  $i_k/i_c$ , where  $i_k$  (catalytic current) is the anodic peak current of the ABTS **1** in the presence of lignin, and  $i_c$  (diffusion current) is the anodic peak current of the ABTS **1** alone.<sup>21, 27, 38</sup> According to this relationship, the catalytic efficiencies of the two oxidised species of ABTS, **2** and **3**, in the presence of liginosulfonate in 15% (v/v) IL/buffer solution were calculated. On this basis, the anodic current corresponding to the ABTS radical cation **2** increased by 5.9-fold and the ABTS dication **3** by 6.7-fold, reflecting that the oxidation capability of ABTS dication **3** is higher than that of the ABTS cation radical **2**.

The absence of the cation radical peak, as well as the presence of only one small reduction peak, were observed on the CVs of liginosulfonate oxidation (1 wt %) by ABTS **1** in the buffer solution (Figure 14). Noticeably, the dication peak rose strongly in the buffer solution and its catalytic efficiency being intensified by 17.6-fold. The strong current increase at 809 mV indicates that

the reaction between ABTS<sup>2+</sup> **3** and lignosulfonate is relatively fast compared to the reaction with ABTS radical cation **2**.

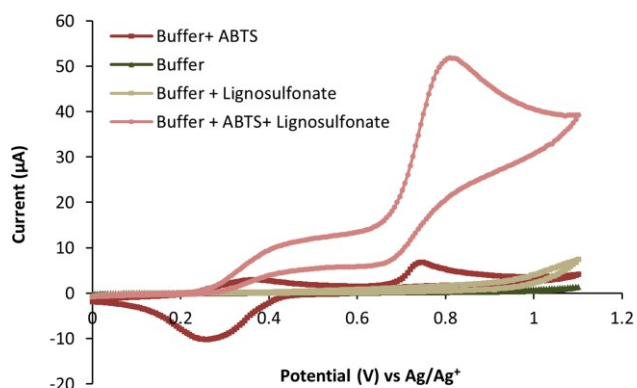


**Figure 14:** Cyclic voltammograms of 1 mM ABTS, 1 wt % lignosulfonate, 1 wt % lignosulfonate mixed with 1 mM ABTS in 0.1 M sodium acetate buffer (pH 4.5) recorded at a scan rate of 10 mV/s.

Electrochemical oxidation of ABTS **1** at a concentration of 1.0 mM was reversible in the buffer solution at the scan rate of 10 mV/s (Figure 13). However, when the scan rate was increased to 400 mV/s, ABTS **1** (1.0 mM) exhibited a more reversible oxidation process (data not shown). This can be explained by the comproportionation reaction between ABTS **1** and its dication **3** to give two equivalents of the radical cation **2** at the slower scan rate. This ABTS behaviour was also found in ionic liquid and discussed previously in the context of the electrochemical oxidation behaviour of ABTS **1** in [C<sub>2</sub>mim][C<sub>2</sub>SO<sub>4</sub>].

It is likely that the viscosity effect could be the reason behind the high increases in anodic peak currents of ABTS **1** in the presence of lignosulfonate in the buffer solution, compared with 15 % (v/v) [C<sub>2</sub>mim][C<sub>2</sub>SO<sub>4</sub>]/buffer solutions, where the viscosity of buffer is around half that of the mixture containing 15 % (v/v) IL (Table 1). Through this decrease in viscosity, a significant increase, about two-fold, in the diffusion coefficient of ABTS **1** in the buffer solution would promote the mass transfer at the electrode surface-bulk solution interface and thus also increase the catalytic efficiencies.

### 3.5 Cyclic Voltammograms of Organosolv Lignin in buffer/[C<sub>2</sub>mim][C<sub>2</sub>SO<sub>4</sub>] Solutions of Different Concentrations

The reaction between the ABTS and organosolv lignin at different concentrations of sodium phosphate buffer (pH 12) in ionic liquid was also explored. As shown in Figure 15, the addition of buffer to the IL resulted in an increase in the second oxidation peak of ABTS **1**. The likely reason behind the initial increase in the dication **3** peak current is a dilution effect, whereby the viscosity of the IL is reduced, resulting in improved mass transfer. This is consistent with the similar electrochemical behaviour seen in solutions of 5 % (v/v) buffer/IL, 7 % (v/v) buffer/IL and 10 % (v/v) buffer/IL, since small quantities of water are known to dramatically affect viscosity. For example, addition of only a 5 % (v/v) of water to [C<sub>2</sub>mim][C<sub>2</sub>SO<sub>4</sub>] could lead to reduction in the IL viscosity by 30 %.<sup>37, 52</sup> Increasing the concentration of phosphate buffer by more than 10 % (v/v) lowered the peak current measured for ABTS **1**. The reduced peak current was most likely

caused by a solubility effect, since the organosolv lignin is insoluble in the sodium phosphate buffer (pH 12). A layer of organosolv lignin could have then formed at the working electrode surface, hence either slowing or preventing ABTS **1** accessing the electrode. These results, taken together, emphasise that viscosity and solubility are important driving factors to consider in lignin-based electrochemical oxidation reactions.

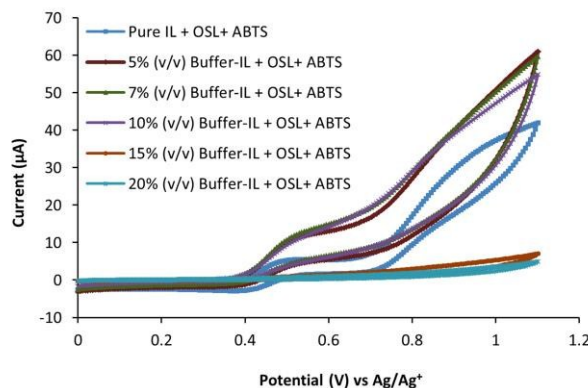


**Figure 15:** Cyclic voltammograms of organosolv lignin (OSL) (5 wt %) mixed with 10 mM ABTS in pure [C<sub>2</sub>mim][C<sub>2</sub>SO<sub>4</sub>], 5 % (v/v) buffer (pH 12)/[C<sub>2</sub>mim][C<sub>2</sub>SO<sub>4</sub>], 7 % (v/v) buffer/[C<sub>2</sub>mim][C<sub>2</sub>SO<sub>4</sub>], 10 % (v/v) buffer/[C<sub>2</sub>mim][C<sub>2</sub>SO<sub>4</sub>], 15 % (v/v) buffer/[C<sub>2</sub>mim][C<sub>2</sub>SO<sub>4</sub>] and 20 % (v/v) buffer/[C<sub>2</sub>mim][C<sub>2</sub>SO<sub>4</sub>] recorded at a scan rate of 50 mV/s.

## Conclusions

Electrochemical oxidation has been explored for the potential degradation of three types of lignin (lignosulfonate, Kraft and organosolv) in [C<sub>2</sub>mim][C<sub>2</sub>SO<sub>4</sub>], utilising the mediator ABTS **1**. The electrochemical behaviour of ABTS **1** alone in [C<sub>2</sub>mim][C<sub>2</sub>SO<sub>4</sub>] was examined and is quite similar to that previously seen in buffered aqueous solutions, in terms of proportionality of peak currents to the square root of the scan rate and the ratio of anodic to cathodic peak currents.

The oxidation currents on the CVs for formation of either or both of the ABTS radical cation **2** and the ABTS dication **3** were observed to increase after addition of all types of lignin, proving ABTS to be an effective mediator for electrochemical oxidation of lignin. However, the use of ABTS was found to affect more significantly the oxidation of organosolv lignin, which is consistent with the greater solubility of this lignin in this IL over the other types of lignin examined in this study. Similarly, solubility of this lignin decreased dramatically at around 10 % (v/v) buffer concentration and resulted in a concomitant reduction in the oxidation peak current.

Solubility of lignin and viscosity of the solvent or solution are likely to play a vital role in the electrochemical oxidation reaction of lignin. The viscosity and interactions of ionic liquid-lignin solutions will influence the mass transfer of ABTS **1** from the electrode surface into the bulk solution, and IL-solute interactions have potential to limit the electron transfer kinetics, as has been shown for other reaction types.<sup>53-55</sup> Overall, the rates of heterogeneous and homogeneous electron-transfer reactions are lower in [C<sub>2</sub>mim][C<sub>2</sub>SO<sub>4</sub>] compared to those measured in the buffer solution. The CV studies of ABTS mediator **1** with lignin demonstrate a high level of catalytic efficiency toward

lignosulfonate in buffer (dication 17.6-fold) and 15% (v/v) [C<sub>2</sub>mim][C<sub>2</sub>SO<sub>4</sub>]/buffer (cation 5.9-fold and dication 6.7-fold) but there was no increase of catalytic efficiency associated with presence of the [C<sub>2</sub>mim][C<sub>2</sub>SO<sub>4</sub>]. A future study investigating the molecular interactions between ABTS/ionic liquid/lignin and lignin/ionic liquid would help to clarify the influence of ionic liquids, both in terms of their solubilisation of lignin components, specific solute-solvent interactions, and viscosity, and delineate their impact on reactivity.

Finally, one of the more significant findings emerging from this study is that the electrochemical techniques can be quickly and easily applied to study ionic liquid/lignin/mediator systems for prediction and selection of an appropriate ionic liquid and mediator combination for the lignin degradation process. This may lead in future to optimised electrochemical processes for improved utilisation of lignolytic biomass in an energy efficient manner.

### Acknowledgements

Majd Eshtaya is grateful to the Islamic Development Bank (IDB) and the University of Nottingham for a doctoral fellowship grant and An-Najah National university for support. AKC acknowledges the support of COST programme CM1206 EXIL. GZC thanks the EPSRC (EP/J000582/1) for funding of the electrochemical equipment used in this work.

### Notes and references

- U. Bornscheuer, K. Buchholz and J. Seibel, *Angew. Chem., Int. Ed.*, 2014, **53**, 10876-10893.
- W. Boerjan, J. Ralph and M. Baucher, *Annu. Rev. Plant Biol.*, 2003, **54**, 519-546.
- G. Chatel and R. D. Rogers, *ACS Sustainable Chem. Eng.*, 2014, **2**, 322-339.
- P. Azadi, O. R. Inderwildi, R. Farnood and D. A. King, *Renewable Sustainable Energy Rev.*, 2013, **21**, 506-523.
- T.-Q. Yuan, F. Xu and R.-C. Sun, *J. Chem. Technol. Biotechnol.*, 2013, **88**, 346-352.
- E. Reichert, R. Wintringer, D. A. Volmer and R. Hempelmann, *Phys. Chem. Chem. Phys.*, 2012, **14**, 5214-5221.
- G. W. Huber, S. Iborra and A. Corma, *Chem. Rev. (Washington, DC, U. S.)*, 2006, **106**, 4044-4098.
- K. Barta, G. R. Warner, E. S. Beach and P. T. Anastas, *Green Chem.*, 2014, **16**, 191-196.
- H. Zhu, L. Wang, Y. Chen, G. Li, H. Li, Y. Tang and P. Wan, *RSC Adv.*, 2014, **4**, 29917-29924.
- A. Toledano, L. Serrano and J. Labidi, *J. Chem. Technol. Biotechnol.*, 2012, **87**, 1593-1599.
- H. Wang, M. Tucker and Y. Ji, *J. Appl. Chem.*, 2013, **2013**, 9.
- A. Hatakka, in *Biopolymers Online*, Wiley-VCH Verlag GmbH & Co. KGaA, 2005, DOI: 10.1002/3527600035.bpol1005.
- F. J. Ruiz-Duenas and A. T. Martinez, *Microb. Biotechnol.*, 2009, **2**, 164-177.
- T. D. H. Bugg, M. Ahmad, E. M. Hardiman and R. Rahmanpour, *Nat. Prod. Rep.*, 2011, **28**, 1883-1896.
- M. Lahtinen, L. Viikari, P. Karhunen, J. Asikkala, K. Kruus and I. Kilpeläinen, *J. Mol. Catal. B: Enzym.*, 2013, **85-86**, 169-177.
- R. Bourbonnais, M. G. Paice, I. D. Reid, P. Lanthier and M. Yaguchi, *Appl. Environ. Microbiol.*, 1995, **61**, 1876-1880.
- D. Rochefort, D. Leech and R. Bourbonnais, *Green Chem.*, 2004, **6**, 14-24.
- R. Bourbonnais and M. G. Paice, *FEBS Lett*, 1990, **267**, 99-102.
- E. Aracri, T. Tzanov and T. Vidal, *Ind. Eng. Chem. Res.*, 2013, **52**, 1455-1463.
- L. P. Christopher, B. Yao and Y. Ji, *Frontiers in Energy Research*, 2014, **2**.
- R. Bourbonnais, D. Leech and M. G. Paice, *Biochimica et Biophysica Acta (BBA) - General Subjects*, 1998, **1379**, 381-390.
- O. V. Morozova, G. P. Shumakovich, S. V. Shleev and Y. I. Yaropolov, *Appl. Biochem. Microbiol.*, 2007, **43**, 523-535.
- D. Rochefort, R. Bourbonnais, D. Leech and M. G. Paice, *Chem. Commun.*, 2002, DOI: 10.1039/b202621j, 1182-1183.
- M. Fabbrini, C. Galli and P. Gentili, *J. Mol. Catal. B: Enzym.*, 2002, **16**, 231-240.
- G. P. Shumakovich, S. V. Shleev, O. V. Morozova, P. S. Khohlov, I. G. Gazaryan and A. I. Yaropolov, *Bioelectrochemistry*, 2006, **69**, 16-24.
- M. Díaz-González, T. Vidal and T. Tzanov, *Appl. Microbiol. Biotechnol.*, 2011, **89**, 1693-1700.
- T. Shiraiishi, Y. Sannami, H. Kamitakahara and T. Takano, *Electrochim. Acta*, 2013, **106**, 440-446.
- A. Kunamneni, F. J. Plou, A. Ballesteros and M. Alcalde, *Recent Pat. Biotechnol.*, 2008, **2**, 10-24.
- M. Lorenzo, D. Moldes, S. Rodríguez Couto and M. Sanromán, *Chemosphere*, 2005, **60**, 1124-1128.
- S. Shipovskov, H. Q. N. Gunaratne, K. R. Seddon and G. Stephens, *Green Chem.*, 2008, **10**, 806-810.
- A. P. M. Tavares, O. Rodriguez and E. A. Macedo, *Biotechnol. Bioeng.*, 2008, **101**, 201-207.
- S. H. Lee, T. V. Doherty, R. J. Linhardt and J. S. Dordick, *Biotechnol. Bioeng.*, 2009, **102**, 1368-1376.
- N. Sun, M. Rahman, Y. Qin, M. L. Maxim, H. Rodriguez and R. D. Rogers, *Green Chem.*, 2009, **11**, 646-655.
- P. Mäki-Arvela, I. Anugwom, P. Virtanen, R. Sjöholm and J. P. Mikkola, *Ind. Crops Prod.*, 2010, **32**, 175-201.
- H. Zhao, *J. Chem. Technol. Biotechnol.*, 2010, **85**, 891-907.
- A. Chen, E. I. Rogers and R. G. Compton, *Electroanalysis*, 2010, **22**, 1037-1044.
- N. Harwardt, N. Stripling, S. Roth, H. Liu, U. Schwaneberg and A. C. Spiess, *RSC Adv.*, 2014, **4**, 17097-17104.

38. K. González Arzola, M. C. Arévalo and M. A. Falcón, *Electrochim. Acta*, 2009, **54**, 2621-2629.
39. H. Liu, L. Zhu, M. Bocola, N. Chen, A. C. Spiess and U. Schwaneberg, *Green Chem.*, 2013, **15**, 1348-1355.
40. K. Stärk, N. Taccardi, A. Bösmann and P. Wasserscheid, *ChemSusChem*, 2010, **3**, 719-723.
41. G. A. Snook, A. S. Best, A. G. Pandolfo and A. F. Hollenkamp, *Electrochem. Commun.*, 2006, **8**, 1405-1411.
42. K. R. J. Lovelock, A. Ejigu, S. F. Loh, S. Men, P. Licence and D. A. Walsh, *Phys. Chem. Chem. Phys.*, 2011, **13**, 10155-10164.
43. S. O'Toole, S. Pentlavalli and A. P. Doherty, *J. Phys. Chem. B*, 2007, **111**, 9281-9287.
44. I. Schroder, E. Steckhan and A. Liese, *J. Electroanal. Chem.*, 2003, **541**, 109-115.
45. A. Rahimi, A. Ulbrich, J. J. Coon and S. S. Stahl, *Nature (London, U. K.)*, 2014, **515**, 249-252.
46. S. Nanayakkara, A. F. Patti and K. Saito, *Green Chem.*, 2014, DOI: 10.1039/c3gc41708e.
47. I. Cybulska, G. Brudecki, K. Rosentrater, J. L. Julson and H. Lei, *Bioresour. Technol.*, 2012, **118**, 30-36.
48. A. George, K. Tran, T. J. Morgan, P. I. Benke, C. Berrueco, E. Lorente, B. C. Wu, J. D. Keasling, B. A. Simmons and B. M. Holmes, *Green Chem.*, 2011, **13**, 3375-3385.
49. R. Bourbonnais and M. Paice, *J. Electrochem. Soc.*, 2004, **151**, E246-E249.
50. A. M. Campos and E. A. Lissi, *Int. J. Chem. Kinet.*, 1997, **29**, 219-224.
51. E. Matsumura, E. Yamamoto, A. Numata, T. Kawano, T. Shin and S. Murao, *Agric. Biol. Chem.*, 1986, **50**, 1355-1357.
52. H. Rodriguez and J. F. Brennecke, *J. Chem. Eng. Data*, 2006, **51**, 2145-2155.
53. H. M. Yau, S. J. Chan, S. R. D. George, J. M. Hook, A. K. Croft and J. B. Harper, *Molecules*, 2009, **14**, 2521-2534.
54. H. M. Yau, S. T. Keaveney, B. J. Butler, E. E. L. Tanner, M. S. Guerry, S. R. D. George, M. H. Dunn, A. K. Croft and J. B. Harper, *Pure Appl. Chem.*, 2013, **85**, 1979-1990.
55. H. M. Yau, S. A. Barnes, J. M. Hook, T. G. A. Youngs, A. K. Croft and J. B. Harper, *Chem. Commun. (Cambridge, U. K.)*, 2008, DOI: 10.1039/b805255g, 3576-3578.